Cannabinoid Receptor-Mediated Modulation of Inhibitory Inputs to Mitral Cells in the Main Olfactory Bulb

Ze-Jun Wang[1*], Sherry Shu-Jung Hu[2*], Heather B. Bradshaw[3], Liqin Sun[1], Ken Mackie[3], Alex Straiker[3], and Thomas Heinbockel[1]

[1]Department of Anatomy, Howard University College of Medicine, Washington, DC 20059, USA; [2]Department of Psychology, National Cheng Kung University, Tainan 701, Taiwan; [3]The Gill Center for Biomolecular Science and the Department of Psychological and Brain Sciences, Indiana University, Bloomington, IN 47405, USA

Author contributions: Z.W., S.H., A.S., and T.H. designed research; Z.W., S.H., H.B., L.S., K.M., A.S., and T.H. performed research; Z.W., S.H., K.M., A.S., and T.H. analyzed data; Z.W., S.H., A.S. and T.H. wrote the paper.

*Z.W. and S.H. contributed to this work to a comparable extent.

Running head: Cannabinoid Receptor-Mediated Modulation of Mitral Cells

Contact Information:

Thomas Heinbockel, Dept. of Anatomy, Howard University College of Medicine, 520 'W' Street, NW, Washington, DC 20059; tel.: (202) 806-9873; fax: (202) 265-7055; email: theinbockel@howard.edu

Non-standard abbreviations: Δ^9-THC, Δ^9-tetrahydrocannabinol; 2-AG, 2-arachidonoyl glycerol; ABHD4/6/12, α/β-hydrolase domain 4/6/12; anandamide or AEA, *N*-arachidonoyl ethanolamine; CB_1 and CB_2, cannabinoid receptor 1 and 2; DGLα/β, diacylglycerol lipase α and β; DHEA, docosahexaenoylethanolamide*;* eCBs, endocannabinoids; EPL, external plexiform layer; GCL, granule cell layer; FAAH, fatty acid amide hydrolase; GDE1, glycerophosphodiesterase 1; GL, glomerular layer; IPL, internal plexiform layer; MCL, mitral cell layer ; MGL, monoacylglycerol lipase; MOB, main olfactory bulb; NAAA, *N*-acylethanolamine-hydrolyzing acid amidase; NAPE-PLD, *N*-acyl phosphatidylethanolamine phospholipase D; OEA, oleoyl ethanolamide; ONL, olfactory nerve layer; PEA, palmitoyl ethanolamide; SEA, stearoyl ethanolamide.

Abstract

The endocannabinoid (eCB) signaling system has been functionally implicated in many brain regions. Our understanding of the role of cannabinoid receptor type 1 (CB_1) in olfactory processing remains limited. Cannabinoid signaling is involved in regulating glomerular activity in the main olfactory bulb (MOB). However, the cannabinoid-related circuitry of inputs to mitral cells in the MOB has not been fully determined. Using anatomical and functional approaches we have explored this question. CB_1 was present in periglomerular processes of a GAD65-positive sub-population of interneurons but not in mitral cells. We detected eCBs in the mouse MOB as well as the expression of CB_1 and other genes associated with cannabinoid signaling in the MOB. Patch-clamp electrophysiology demonstrated that CB_1 agonists activated mitral cells and evoked an inward current, while CB_1 antagonists reduced firing and evoked an outward current. CB_1 effects on mitral cells were absent in subglomerular slices in which the olfactory nerve layer and glomerular layer were removed, suggesting the glomerular layer as the site of CB_1 action. We previously observed that GABAergic periglomerular cells show the inverse response pattern to CB_1 activation compared to mitral cells, suggesting that CB_1 indirectly regulates mitral cell activity as a result of cellular activation of glomerular GABAergic processes . This hypothesis was supported by the finding that cannabinoids modulated synaptic transmission to mitral cells. We conclude that CB_1 directly regulates GABAergic processes in the glomerular layer to control GABA release and, in turn, regulates mitral cell activity with potential effects on olfactory threshold and behavior.

New & Noteworthy

Cannabinoid signaling with cannabinoid receptor type 1 (CB_1) is involved in the regulation of glomerular activity in the main olfactory bulb (MOB). We detected endocannabinoids in the mouse MOB. CB_1 was present in periglomerular processes of a GAD65-positive sub-population of interneurons. CB_1 agonists activated mitral cells. CB_1

directly regulates GABAergic processes to control GABA release and, in turn, regulates mitral cell activity with potential effects on olfactory threshold and behavior.

Key Words: Cannabinoid; patch-clamp; sIPSC; AM251; WIN 55,212-2; CB_1; glomerulus, GAD65, GAD67, gene expression, lipid measurement

Introduction

The endocannabinoid system has emerged as an important neuromodulatory system (Ianotti et al., 2016), which involves cannabinoid receptors, CB_1 and CB_2, and their endogenous activators, the endocannabinoids (eCBs). Immunohistochemical and autoradiographic studies indicate that CB_1 is present in the main olfactory bulb (MOB) with moderate to intense levels of staining (Herkenham et al. 1991; Pettit et al. 1998; Tsou et al. 1998; Moldrich and Wenger 2000). Moldrich and Wenger (2000) observed a moderate density of CB_1 immunoreactive cell bodies and fibers in several layers of the MOB: glomerular layer, mitral cell layer, internal plexiform layer, granule cell layer. In the granule cell layer, CB_1 is abundantly expressed on axon terminals of centrifugal cortical glutamatergic neurons that project to inhibitory granule cells (Soria-Gomez et al., 2014).

Many CB_1 expressing neurons in the CNS are GABAergic (Tsou et al. 1998). Functionally, eCBs can act on CB_1 at presynaptic terminals to reduce transmitter release, diminishing glutamate (Levenes et al. 1998; Takahashi and Linden 2000; Kreitzer and Regehr 2001a) and GABA release (Katona et al. 1999; Hoffman and Lupica 2000; Ohno-Shosaku et al. 2001; Varma et al. 2001; Wilson and Nicoll 2001; Diana et al. 2002) in the hippocampus and cerebellum. Two eCBs are strongly implicated in cannabinoid signaling, 2-arachidonoyl glycerol (2-AG, Sugiura et al., 1995; Mechoulam et al., 1995) and arachidonoyl ethanolamine (AEA, anandamide, Devane et al., 1992). These lipid messengers are produced and broken down enzymatically. Intriguingly, cannabinoid signaling in the MOB is implicated in regulating appetite and olfactory threshold through centrifugal fiber input to inhibitory granule cells as a means of cortical feedback to the MOB (Soria-Gomez et al., 2014; Pouille and Schoppa, 2018). However, little is known about the relevance of CB_1 for mitral cell activity in MOB glomeruli.

The MOB is the first central relay station for olfactory information conveyed from the nasal epithelium by olfactory receptor neurons. Sensory transmission from olfactory nerve terminals to principal neurons of the MOB, mitral and tufted cells, is regulated by

juxtaglomerular cells in glomeruli. Several types of neurons collectively referred to as juxtaglomerular cells send dendrites into the glomerular neuropil (reviewed in Ennis et al., 2007) targeting external tufted cells, 'short axon' cells, and periglomerular cells. Cells in the glomerular layer express NAPE-PLD, an enzyme implicated in the synthesis of anandamide (Egertova et al., 2008; Okamoto et al 2007) but the Allen Brain Atlas shows little message for the 2-AG-synthesizing enzymes diacylglycerol lipase alpha (DAGLα) or beta (DAGLβ). Periglomerular cells are GABAergic interneurons while external tufted cells are glutamatergic (Ribak et al. 1977; Hayar et al., 2004b; Kiyokage et al., 2010). Periglomerular cells receive input from the olfactory nerve or dendrodendritic glutamatergic input from external tufted or mitral cells (Pinching and Powell 1971; Shipley and Ennis 1996; Hayar et al., 2004b; Ennis et al., 2007). Through GABAergic transmission, periglomerular cells presynaptically inhibit olfactory receptor neurons (Aroniadou-Anderjaska et al., 2000; Murphy et al., 2005) and postsynaptically regulate mitral cell activity (Dong et al., 2007). Short axon cells express both GABA and dopamine and form extensive interglomerular connections (Kiyokage et al., 2010).

To study the function of the eCB system in the MOB, we determined cannabinoid levels and the expression of CB_1 and other genes associated with the cannabinoid signaling system in the MOB. We additionally tested the effects of agonists/antagonists of CB_1 on cellular and network activity of a key neuronal cell type, mitral cells, in a slice preparation of the mouse MOB.

Materials and Methods

Animal use

All procedures used in this study were approved by the Animal Care Committees of Howard University, Indiana University and National Cheng Kung University and conform to the Guidelines of the National Institutes of Health on the Care and Use of Animals.

Immunohistochemistry

Adult mice (CD1 strain (4), C57/BL6 strain (4), CB_1 KO on CD1 strain (2), GAD67 strain on C57/BL6 strain (2), >5 weeks, of either sex, from breeding colony) were housed under a 12/12 hour day/night cycle. Mice were perfused transcardially under deep isoflurane anesthesia first with 0.9% saline and then with 4% paraformaldehyde dissolved in phosphate buffer (PB) at 4°C. After perfusion, the MOB was removed from the skull and further fixed in 4% paraformaldehyde solution for 1 hour followed by a 30% sucrose immersion for 24-72 hours at 4°C. Tissue was then rapidly frozen in TissueTek OCT (optimum cutting temperature) compound and sectioned (15-20 μm) using a Leica CM1850 cryostat (Leica Biosystems). Tissue sections were mounted onto Superfrost-Plus slides, washed, treated with Sea Block blocking buffer (Thermo Fisher Scientific) for 30 minutes, afterwards with primary antibodies prepared in PBS with a detergent (Triton-X100, 0.3% or saponin, 0.1%) and incubated overnight at 4°C. Secondary antibodies (Alexa647, Alexa594 or Alexa488, 1:500, Invitrogen) were subsequently applied at room temperature for 1.5 hours. Finally, sections were washed three times with 0.1 M PBS, twice with 0.1 M PB, and three times with water and air-dried. Coverslips were mounted on top of these sections with a drop of Vectashield containing DAPI (Vector Laboratories,Inc.). Sections were examined with a Leica TCS SP5 confocal microscope. Images were processed by ImageJ (freeware, available at https://imagej.nih.gov/ij/) and/or Photoshop (Adobe Systems). Images were only modified in terms of brightness and/or contrast.

GAD67-GFP mice generated by Dr. Yuchio Yanagawa (Gunma University, Gunma, Japan (Tamamaki *et al.*, 2003)) were provided by Dr. Albert Berger (University of Washington, Seattle WA), with Dr. Yanagawa's permission.

Antibody Characterization

The specificity of CB_1-L15 has been previously characterized by using knockout mouse models and the immunostaining for CB_1 was completely absent in the corresponding knockout (Bodor *et al.*, 2005; Bracey *et al.*, 2002; Hajos *et al.*, 2000) in those studies and also in this manuscript (Fig. 1B). The specificity of the GAD65 antibody (mouse monoclonal, 1:600; Developmental Studies Hybridoma Bank) was established by the recognition of a single band of 64 kDa (representing glutamic acid decarboxylase (GAD)) by Western blotting (Chang *et al.*, 1988; Jevince *et al.*, 2006). The recoverin antibody (Rabbit, polyclonal, 1:1000; Chemicon catalog number AB5585) recognized a 25 kDa band on Western blots of mouse retina (Hendrickson *et al.*, 2009).

Quantification of basal levels of 2-AG, AEA, and related acyl amides in murine OB

16 mice were euthanized by rapid cervical dislocation and olfactory bulbs were dissected and fresh-frozen in liquid nitrogen prior to lipid extraction to test the basal levels of 2-AG, AEA and other related acyl amides (e.g., OEA, PEA, SEA, and DHEA). Each of the analytes was extracted and quantified using methods previously described (Bradshaw *et al.*, 2009; Hu *et al.*, 2008). In brief, twenty volumes of ice-cold HPLC-grade methanol and 100 pmol D_8AEA (internal standard) were added to the methanol-tissue sample. The samples were maintained on ice and sonicated for 1 min and centrifuged at 19000 x g at 24°C for 20 min. Supernatants were collected and HPLC-grade water was added to a final concentration of 25% methanol. Bond–Elut cartridges (100 mg C18) were conditioned with 5 ml methanol and 3 ml water. The extract was then loaded and passed through by gentle, low-pressure aspiration. After washing with 5

ml water and 2 ml of 40% methanol, the following fractions were collected and analyzed via HPLC/MS/MS: 60%, 75%, 85%; and 100% methanol. Mass spectrometric analysis was performed with an Applied Biosystems/MDS Sciex (Foster City, CA) API3000 triple quadrupole mass spectrometer using electrospray ionization. Eluents were tested for levels of 2-AG, AEA, related acyl amides as previously described (Leishman et al. 2016a, b).

Examination of the expression of cannabinoid-related genes in murine OB by reverse transcription and polymerase chain reaction (RT-PCR)

The sequences of primers designed against CB_1 and 11 additional cannabinoid-related mouse genes (CB_2, NAPE-PLD, ABHD4, GDE1, FAAH, NAAA, DGLα, DGLβ, MGL, ABHD6, ABHD12) are listed on Table 1. GAPDH is a housekeeping gene used as an internal control. Expression of mRNAs was determined by RT-PCR. Total RNA was isolated from OB using Trizol reagent (Life Technologies, NY) and RNeasy Kit (Qiagen, Valencia, CA) according to the manufacturer's instructions. RT-PCR was carried out in two steps. The first strand DNA was made using High Capacity RNA-to-cDNA Kit (Applied Biosystems, Foster City, CA) using 200 ng RNA in a 20 µl reaction. PCR was performed following the AmpliTaq 360 DNA Polymerase Protocol (Applied Biosystems, Foster City, CA). 1 µl respective mouse OB cDNA was added into a 25 µl PCR reaction that was processed through 40-cycle amplification. PCR products were examined on 1% agarose gel stained with ethidium bromide (EtBr).

Slice preparation

Wildtype mice of either sex (C57BL/6J, Jackson Laboratory, Bar Harbor, ME) were used. Juvenile (16–25 day old) mice were decapitated, and the MOBs were dissected out and immersed in artificial cerebrospinal fluid (ACSF, see below) at 4ºC, as previously described (Heinbockel et al., 2004). Horizontal slices (400 µm-thick) were cut parallel to the long axis using a vibratome (Vibratome Series 1000, Ted Pella Inc., Redding, CA). For recording, a brain

193 slice was placed in a recording chamber mounted on a microscope stage and maintained at 30
194 ± 0.5°C by superfusion with oxygenated ACSF flowing at 2.5–3 ml/min.
195
196 ***Electrophysiology***
197 Visually-guided recordings were obtained from cells in the mitral cell layer with near-infra
198 red differential interference contrast optics and a BX51WI microscope (Olympus Optical, Tokyo,
199 Japan) equipped with a camera (C2400-07, Hamamatsu Photonics, Japan). Images were
200 displayed on a Sony Trinitron Color Video monitor (PVM-1353MD, Sony Corp. Japan).
201 Recording pipettes (5-8 MΩ were pulled on a Flaming-Brown P-97 puller (Sutter Instrument Co.,
202 Novato, CA) from 1.5 mm O.D. borosilicate glass with filament. Seal resistance was routinely
203 >1GΩ and liquid junction potential was 9-10 mV; reported measurements were not corrected for
204 this potential. Data were obtained using a Multiclamp 700B amplifier (Molecular Devices,
205 Sunnyvale, CA). Signals were low-pass Bessel filtered at 2 kHz and digitized on computer disc
206 (Clampex 10.1, Molecular Devices). Data were also collected through a Digidata 1440A
207 Interface (Molecular Devices) and digitized at 10 kHz. Holding currents were generated under
208 control of the Multiclamp 700B Commander. Membrane resistance was calculated from the
209 amount of steady-state current required to hyperpolarize the cell by 10 mV, typically from -60
210 mV to -70 mV. The detection of events (intracellularly recorded spontaneous inhibitory
211 postsynaptic currents, sIPSCs) and spontaneous excitatory postsynaptic currents (sEPSCs)
212 was performed off-line using Mini Analysis program (Synaptosoft, Decatur, GA).
213 Membrane potentials were calculated from the steady-state membrane potential that
214 occurred after a single action potential. Minimal membrane potential was measured as
215 membrane potential for burst firing (Liu and Shipley, 2008). To reduce the variance of
216 spontaneous mitral cell firing rate, mitral cells with firing rates of 2-6 Hz were used for testing
217 cannabinoid actions. Numerical data were expressed as the mean ± SEM. Tests for statistical
218 significance ($p < 0.05$) were performed using paired Student's *t*-test, and non-parametric

Wilcoxon signed rank test for paired data of small sample sizes (~5), or one-way ANOVA followed by the Bonferroni test for multiple comparisons.

The ACSF consisted of (in mM): NaCl 124, KCl 3, $CaCl_2$ 2, $MgSO_4$ 1.3, glucose 10, sucrose 4.4, $NaHCO_3$ 26, NaH_2PO_4 1.25 (pH 7.4, 300 mOsm), saturated with 95 O_2/5% CO_2 (modified from Heyward et al. 2001). For intracellular recording of spiking activity, the pipette-filling solution consisted of (mM) K-gluconate 144, $MgCl_2$ 2, HEPES 10, Mg_2ATP 2, Na_3GTP 0.2, NaCl 2, EGTA 0.2. Lucifer yellow (0.02%, Molecular Probes) was added to the intracellular solution in a subset of experiments for *in situ* and *post hoc* labeling, respectively. We observed no difference in neuronal properties and behavior when Lucifer Yellow was included in the recording pipette. For intracellular recordings of IPSCs, EPSCs, electrodes were filled with a high-Cl^- or low-Cl^--based solution depending on the purpose of experiments. High-Cl^--based pipette solution contained the following composition (in mM): 110 cesium cloride, 10 tetraethylammonium-Cl, 2 NaCl, 10 phosphocreatine ditris salt, 2 MgATP, 0.3 GTP, 0.5 EGTA, 10 HEPES, 10 QX-314 [2(triethylamino)-N-(2,6-dimethylphenyl) bromide], pH 7.3 with 1N CsOH (osmolarity, 290 Osm). Low-Cl^--based pipette solution contained the following composition (in mM): 125 cesium methanesulfonate ($CsMeSO_3$), 1 NaCl, 10 phosphocreatine ditris salt, 2 MgATP, 0.3 GTP, 0.5 EGTA, 10 HEPES, 10 QX-314 [2(triethylamino)-N-(2,6-dimethylphenyl) bromide], pH 7.3 with 1N CsOH (osmolarity, 290 Osm).

The following drugs were bath applied: L-2-amino-5-phosphonopentanoic acid (AP5, APV), 6-cyano-7-nitroquinoxaline-2-3-dione (CNQX), (2-(3-carboxypropyl)-3-amino-6-(4 methoxyphenyl)-pyridazinium bromide (gabazine, SR-95531), (*R*)-(+)-[2,3-Dihydro-5-methyl-3-(4-morpholinylmethyl)pyrrolo[1,2,3,-de]-1,4-benzoxazin-6-yl]-1-naphthalenylmethanone mesylate (WIN55,212-2 mesylate), *N*-(Piperidin-1-yl)-5-(4-iodophenyl)-1-(2,4-dichlorophenyl)-4methyl-1*H*-pyrazole-3-carboxamide (AM251), (1*R*,4a*S*,10a*R*)-1,2,3,4,4a,9,10,-Octahydro-1-4a-dimethyl-7-(1-methylethyl)-1-phenanthrenemethanamine hydrochloride (Leelamine hydrochloride, Lylamine hydrocholoride), *N*-(2-Hydroxyethyl)-5*Z*,8*Z*,11*Z*,14*Z*-

245 eicosatetraenamide (Anandamide, AEA), 5-(4-Chlorophenyl)-1-(2,4-dichloro-phenyl)-4-methyl-
246 *N*-(piperidin-1-yl)-1*H*-pyrazole-3-carboxamide (SR141716, Rimonabant). Chemicals and drugs
247 were supplied by Sigma-Aldrich (St. Louis, MO) and Tocris (Ellisville, MO), except for
248 SR141716 which was supplied by the NIDA Drug Inventory Supply and Control System.
249
250

Results

CB_1 is present in periglomerular processes of a GAD65-positive sub-population of interneurons

To delineate the receptor expression of CB_1 we made use of an antibody against the last 15 residues of the CB_1 receptor. In the glomerular, external plexiform and mitral cell layer of the MOB we observed staining tightly restricted to neuron-like processes in the glomerular layer (Fig. 1A). This staining was absent in the same regions of the MOB taken from $CB_1^{-/-}$ mice (Fig. 1B). Occasional processes were seen to extend into the external plexiform layer, perhaps representing the origin of these processes. The staining was periglomerular in nature as demonstrated by our co-staining with recoverin, which outlines glomeruli (Fig 1D). Apart from rare processes in the external plexiform layer, no pronounced staining was observed in the external plexiform or mitral cell layer (Fig. 1E). To identify the population of neurons that express CB_1, we tested CB_1 staining against markers of interneuron populations using tissue from GAD67-GFP reporter mice (e.g. Fig 1A) or an antibody against GAD65. Using this approach, we found that CB_1 colocalizes with a small subset of GAD65-positive interneurons (Fig. 1F,G). We did not observe staining of neuronal somas, perhaps an indication that the CB_1 staining is restricted to neuronal processes.

The endocannabinoid 2-AG and other related lipids are detected in the mouse MOB

Cannabinoid receptors are lipid receptors, known to be activated by endogenous cannabinoids 2-arachidonoyl glycerol (2-AG, (Stella *et al.*, 1997)) and anandamide (AEA, (Devane *et al.*, 1992)). These are part of a larger family of lipids that have been hypothesized to play physiological roles in the body (Piomelli, 2003). We tested for the presence of 2-AG, AEA, and several other related lipids in the MOB (Fig. 2A-F). We found that 2-AG levels were the highest among those tested, consistent with its hypothesized role as a CB_1 receptor ligand. At ~2 nmoles/g of tissue, 2-AG levels are comparable to if somewhat lower than those seen

elsewhere in the brain (Stella *et al.*, 1997). AEA levels were considerably lower (the lowest of the six lipids tested), though this is also consistent with findings for other regions of the brain (Cravatt *et al.*, 2001). Interestingly, oleoyl ethanolamide (OEA) levels, at 100 pmoles/g were lower than reported for brain (Oveisi *et al.*, 2004) yet considerably higher than those for palmitoyl ethanolamide (PEA). Low levels of stearoyl ethanolamide (SEA) and docosahexaenoyl ethanolamide (DHEA) were also detected.

Expression of cannabinoid-related genes in the mouse main olfactory bulb by RT-PCR

As a complementary assay, we tested for mRNA expression of a wide range of cannabinoid-related proteins (CB_1, CB_2, NAPE-PLD, ABHD4, GDE1, FAAH, NAAA, DGLα, DGLβ, MGL, ABHD6, ABHD12) in the mouse MOB. This allowed independent verification of immunohistochemistry results for CB_1 and also allowed us to obtain data regarding the expression of a multiplicity of other genes known or suspected to be associated with the cannabinoid signaling system.

Our results suggest that all of the components of cannabinoid signaling are present in the mouse MOB (Fig. 3). As expected, high levels of CB_1 mRNA were present. However, the level of CB_2 mRNA is very close to our detection limit. Expression patterns of the enzymes involved in AEA and 2-AG biosynthesis (e.g., NAPE-PLD, ABHD4, GDE1 for AEA; DGLα/β for 2-AG) and metabolism (e.g., FAAH and NAAA for AEA; MGL and ABHD6/12 for 2-AG) were almost all present in the mouse MOB, although the expression of MGL mRNA is relatively low compared to ABHD6/12. Taken together with the immunohistochemistry results, these data indicate that the murine MOB is well-supplied with known and hypothesized enzymes for the synthesis/metabolism of AEA and 2-AG.

CB_1 agonists and antagonist modulate mitral cell membrane potential and firing rate

To determine the functional relevance of CB_1 in MOB neural circuits, we recorded from 203 mitral cells in mouse MOB slices. Mitral cells were identified visually by their soma location and relatively large soma size, and by their input resistance (284 ± 16.6 MΩ, *n* = 69). The membrane potential of mitral cells in this study was -50.5 ± 0.6 mV (*n* = 69).

We first tested if selective and non-selective agonists of CB_1 regulate the activity of mitral cells in current clamp recording conditions. Specifically, we tested whether CB_1 agonists can affect the firing rate and membrane potential of mitral cells. Mitral cells exhibited a background action potential firing rate ranging from 1 to 8 Hz (Heinbockel et al. 2004). The selective CB_1 agonist anandamide (AEA, 10 μM) increased their firing rate (control firing rate: 3.48 ± 0.58 Hz vs. in AEA: 4.51 ± 0.74 Hz, n = 10, $p < 0.05$) (Fig. 4A) and depolarized mitral cells (ΔVm = 2.5 ± 0.5 mV, n = 11, $p < 0.001$) (Fig. 4B).

Similar excitatory effects on mitral cell firing rate were seen in response to bath application of CB_1 agonist WIN 55,212-2 mesylate (WIN552122, WIN, 1μM) (control: 3.71 ± 0.59 Hz vs. in WIN: 5.27 ± 0.71 Hz, n = 10, $p < 0.01$), CP 55,940 (control: 3.75 ± 0.76 Hz vs. in CP, 1 μM: 5.28 ± 0.86 Hz, n = 6, $p < 0.05$).The effects of the two CB_1 agonists on firing rate and membrane potential of mitral cells were not significantly different from each other ($p > 0.05$ determined by ANOVA and Bonferroni post-hoc analysis; firing rate: $p = 0.83$; Vm: $p = 0.28$).

To test if the above excitatory effects were mediated by CB_1 we bath applied the selective CB_1 antagonists AM251. AM251 (10 μM) hyperpolarized mitral cells (ΔVm = -0.9 ± 0.2 mV, n = 19, $p < 0.001$) (Fig. 4D) and markedly reduced their firing rate (Fig. 4C,E; control: 4.12 ± 0.65 Hz vs. in AM251: 3.06 ± 0.56 Hz, n = 19, $p < 0.001$). We further tested if the effects of WIN were CB_1-dependent by pretreating cells with the CB_1 antagonist AM251. In the presence of 10 μM AM251, bath application of WIN failed to induce an increase in firing rate (in AM251: 3.13 ± 0.75 Hz vs. in AM251 plus WIN: 3.07 ± 0.77 Hz, n = 6, $p > 0.05$) or change in membrane

potential (in AM251 plus WIN, ΔVm = 0.2 ± 0.3 mV, n = 11, $p > 0.05$). These results indicate that CB_1 was involved in cannabinoid-mediated modulation of mitral cell activity.

CB_1 agonist and antagonist modulate synaptic transmission in mitral cells

As the next step, we wanted to determine if spontaneous GABAergic inputs from periglomerular cells to mitral cells might be the target of CB_1-mediated modulation. Our electrophysiological and anatomical data are consistent with CB_1-mediated modulation of periglomerular GABAergic interneurons. In this model, changes in mitral cell activity are due to modulation of GABAergic interneuron signaling in the MOB. Excitatory inputs and/or inhibitory synaptic transmission originating from GABAergic interneurons such as periglomerular cells could therefore modulate mitral cell activity. Therefore, we tested the effect of CB_1 agonists and an antagonist on GABAergic spontaneous inhibitory postsynaptic currents (sIPSCs).

Using a low-Cl^- pipette solution in voltage-clamp mode at a holding potential of 0 mV, we observed sIPSCs in a subset of mitral cells. Fig. 5A shows the increase of sIPSCs in response to CB_1 antagonist AM251 in a representative mitral cell. sIPSCs in mitral cells were outwardly directed in this condition. To examine sIPSCs in mitral cells more easily, a high-Cl^--based pipette solution was used to observe changes in sIPSCs (Wang et al., 2012). sIPSCs in mitral cells were directed downward in this condition and could be completely blocked by 10 μM gabazine, indicating that the currents were mediated by $GABA_A$ receptors. Fig. 5B shows that CB_1 antagonist AM251 increased the frequency of sIPSCs in the presence of CNQX plus AP5 in a representative mitral cell. Ionotropic glutamate receptor blockers (CNQX plus AP5) reduced the frequency of sIPSCs (data not shown). In mitral cells, bath application of 10 μM AM251 increased the frequency of sIPSCs (in CNQX + AP5: 1.7 ± 0.4 Hz; in CNQX + AP5 plus AM251: 2.3 ± 0.4 Hz, n = 7, $p < 0.05$), and evoked outward currents of 13.3 ± 6.4 pA (n = 7, range 4.5 - 27 pA) which is consistent with the inhibitory effect of AM251 on mitral cells (Fig. 4D, F). Fig.

5C shows that the CB_1 agonist WIN reduced the sIPSCs frequency in a mitral cell in the presence of CNQX plus AP5. Bath application of WIN (1 μM) decreased the frequency of sIPSCs (in CNQX + AP5: 1.5 ± 0.1 Hz; in CNQX + AP5 plus WIN: 1.2 ± 0.1 Hz, n = 5, $p < 0.01$), and evoked inward currents of 21.6 ± 7.3 pA ($n = 5$). The results suggest that cannabinoids synaptically regulate mitral cell activity by regulating GABA release from interneurons.

The modulation of sIPSCs by cannabinoids was also tested in subglomerular slices in which the olfactory nerve layer and glomerular layer were removed (Dong et al. 2007), see also below. In subglomerular slices, WIN did not modulate sIPSC frequency (0.9 ± 0.08 Hz vs. in WIN: 0.9 ± 0.07 Hz, n = 5, $p > 0.05$) or evoke inward currents in mitral cells (ΔI = 3.8 ± 0.3 pA, n = 12, $p > 0.05$). The failure of WIN to modulate sIPSC frequency and inward currents in mitral cells in subglomerular slices supported the idea that stimulation of periglomerular GABAergic processes modulated mitral cell activity through CB_1 activation.

Cannabinoids failed to modulate mitral cell activity in subglomerular slices

Several types of GABAergic interneurons in the MOB express CB_1 (Moldrich and Wenger 2000) and, potentially, can be regulated through direct activation of CB_1. Periglomerular cells are likely candidates for direct effects of cannabinoids since CB_1 is robustly expressed in the glomerular layer of the MOB (Fig. 1 and Moldrich and Wenger, 2000). Periglomerular cells form a heterogeneous neuron population with different firing patterns and morphological properties (Shao et al. 2009; Kiyokage et al. 2010). We previously reported that a CB_1 agonist inhibited periglomerular cells whereas a CB_1 antagonist activated them (Wang et al., 2012), i.e. the inverse response pattern to CB_1 activation compared to mitral cells (Fig. 4). These findings suggested that CB_1 indirectly regulated mitral cell activity by modulating inhibitory inputs to mitral cells.

Potentially, another type of GABAergic interneuron was regulated by CB_1, in addition to periglomerular cells, namely granule cells in the granule layer. To determine if one or both GABAergic interneuron types played a role in mitral cell regulation we used a subglomerular slice preparation in which the olfactory nerve layer and glomerular layer were removed (Dong et al. 2007). Mitral cell properties in subglomerular slices (Vm, input resistance, spike rates) were not significantly different from mitral cells in intact MOB slices (Vm: -49.5 ± 1.7 mV, input resistance: 299 ± 42.1 MΩ, spike rates: 1 to 8 Hz; *n* = 18).

In subglomerular slices, WIN failed to depolarize mitral cells (Fig. 6). Compared to control conditions, in subglomerular slices WIN did not change the frequency of spiking (control: 4.58 ± 0.50 Hz vs. in WIN: 4.47 ± 0.46 Hz, n = 12, $p > 0.05$) or the membrane potential of mitral cells (ΔVm = 0.1 ± 0.2, n = 12, $p > 0.05$). Correspondingly, AM251 failed to decrease the frequency of mitral cell spiking in subglomerular slices (control: 4.00 ± 0.61 Hz vs. in AM251: 4.11 ± 0.62 Hz, n = 7, $p > 0.05$) or change the membrane potential (ΔVm = 0.3 ± 0.1, n = 7, $p > 0.05$). These results suggested the involvement of periglomerular cells in CB_1-mediated mitral cell modulation in the glomerular layer and ruled out granule cells as modulators of mitral cell activity through CB_1 activation.

CB_1 effects are eliminated in blockers of fast synaptic transmission

One potential alternative explanation for the results is that they occur via activation of CB_1 expressed by mitral cells, which would directly affect the output of mitral cells rather than their input. Similar response profiles have been seen with other G-protein coupled receptors expressed on mitral cells, e.g., mGluRs (Heinbockel et al. 2004). Previously, mitral cells were shown to express CB_1 at a low level (Moldrich and Wenger 2000). However, our immunohistochemical data suggest an extra-mitral site of action. For example, cannabinoids could activate CB_1 expressed by other MOB cell types such that the observed excitatory and

401 inhibitory effects of CB_1 agonists and antagonists on mitral cells were indirect. Therefore, we
402 applied a CB_1 agonist and antagonist in the presence of blockers of GABAergic and ionotropic
403 glutamatergic transmission (fast synaptic blockers) (Fig. 7A, B).
404 Fast synaptic blockers, which included blockers of ionotropic glutamate and $GABA_A$
405 receptors (CNQX, 10 μM; AP5, 50 μM; gabazine, 5 μM), did not significantly change the regular
406 firing rate and membrane potential (for the firing rate: 109.1 ± 10.0% of control, n = 20, $p > 0.05$,
407 paired *t* test; for the membrane depolarization: ΔVm = 0.3 ± 0.1 mV, n = 20, $p > 0.05$, paired *t*
408 test). In the presence of fast synaptic blockers, AM251 (10 μM) failed to significantly decrease
409 the firing rate (in synaptic blockers: 3.66 ± 0.64 Hz vs. in synaptic blockers plus AM251: 3.74 ±
410 0.75 Hz, n = 9, $p > 0.05$) or change the membrane potential of mitral cells (ΔVm = 0.2 ± 0.3 mV,
411 n = 9, $p > 0.05$). Blockade of the AM251-evoked inhibitory effect by fast synaptic blockers
412 indicated that CB_1-mediated regulation of mitral cell activity involved GABAergic and/or
413 glutamatergic synaptic transmission (Fig. 5B). WIN also failed to induce an increase in firing
414 rate (syn. blockers: 4.01 ± 0.72 Hz vs. plus WIN: 3.95 ± 0.88 Hz, n = 7, $p > 0.05$) or membrane
415 potential in the presence of fast synaptic blockers (ΔVm = 0.3 ± 0.4 mV, n = 7, $p > 0.05$) (Fig.
416 7A). These data suggest an indirect effect of CB_1 on mitral cells. The modulation of mitral cell
417 activity could occur not through CB_1 on mitral cells but rather through an indirect effect of
418 cannabinoids, namely on GABAergic processes in the glomerular layer.
419
420
421
422
423
424 **Discussion**

Our chief finding is that activity of mitral cells, the chief output neurons of the olfactory bulb, is regulated in a CB1-dependent manner by a periglomerular interneuron network, likely based in a small subset of GAD65-positive neurons. This offers additional evidence that olfactory sensory inputs to the brain are modulated by the cannabinoid signaling system.

Using immunohistochemistry, we show that CB_1 is expressed in a GAD65-expressing subpopulation of interneurons. The CB_1 expression extended along the processes of these neurons, with a distribution restricted to the periglomerular region of the glomerular zone. The rare processes extending from the external plexiform layer may be an indication that this is where the soma resides. Knockout controls lend confidence to our immunohistochemistry staining and may account for the differences between our observed staining and that previously reported by Moldrich and Wenger 2000.

Our eCB measurements yielded evidence for the presence of CB_1 agonist 2-AG, consistent with the findings of Soria-Gomez et al (2014). The levels are at the low end of the spectrum of values reported for brain, but this may be consistent with the highly restricted expression of CB_1. Levels may also vary depending on stimulation or diurnally (Valenti *et al.*, 2004). Other lipids were also detected but on the low side. For instance, AEA levels were detectable but quite low though AEA levels have typically been found to be lower than those for 2-AG – for instance an early 2-AG study found 2-AG levels to be >170x higher than AEA in brain (Stella *et al.*, 1997). Much evidence for CB_1 signaling in neurons points toward 2-AG (Tanimura *et al.*, 2010) but recent evidence also points to roles for AEA (e.g., Puente et al., 2011), though it should be noted that AEA has also been found to be a full agonist at TRPV1 (Smart *et al.*, 2000). To avoid that the AEA effect is due to TRPV-1 activation in mitral cells (Fig.4), the CB1 agonist WIN was used for subsequent experiments.

Using PCR, we found that many of the identified components of cannabinoid signaling are present in the MOB of the mouse. These proteins for these genes are mostly enzymes involved in production or breakdown of cannabinoids or related lipids. The functional roles of

some of these enzymes (e.g. ABHD4) have not been clearly delineated. The most surprising result is the low expression of MGL. Genetic deletion of this enzyme has been shown to dramatically increase 2-AG levels in the brain of the mouse (Pan *et al.*, 2011). However, there are other enzymes capable of breaking down 2-AG, such as ABHD6 and ABHD12 (Blankman *et al.*, 2007) and it is possible that different brain regions and circuits express a differential complement of 2-AG hydrolyzing enzymes. In addition, the MGL mRNA expression may not correspond to protein levels.

The question of whether CB_2 is expressed in the brain remains controversial. CB_2 has long been associated with the immune system, but there is now some evidence of CB_2 presence in the CNS (reviewed in Atwood and Mackie, 2010). The signal for CB_2 is at the limit of detection for our assay and is, as such, ambiguous, and may be accounted for by low levels of immune-related cells that have intruded into our sample.

CB_1 effects on mitral cells and GABAergic cells in the glomerular layer

Cannabinoids have regulatory effects on principal neurons and interneurons in the MOB. This is different from the hippocampal eCB system where bath application of cannabinoid agonist and antagonist does not lead to significant changes of interneuron membrane properties; the difference may be due to potent enzymatic machinery in the hippocampus that eliminates cannabinoids from the extracellular space (Alger 2002). Effects of cannabinoids on interneurons are typically seen as changes in synaptic transmission from interneurons onto principal neurons, e.g., a reduction of GABA release is reflected as a change in postsynaptic responses of principal neurons (Alger 2002). Our data point to a distinct reduction in firing and membrane hyperpolarization in response to CB_1 activation.

Cannabinoids synaptically modulate mitral cell activity

476 Our results do not suggest that activation and inhibition of CB_1 expressed by mitral cells
477 mediates the CB_1 effects as has been shown for direct actions of other G-protein coupled
478 receptors on mitral cells, e.g., mGluRs (Heinbockel et al. 2004). Mitral cells have been
479 postulated to express CB_1 (Moldrich and Wenger 2000). However, that study, making use of rat
480 tissue, did not have the advantage of murine knockout controls, and our data presented here
481 does not show CB_1 staining in mitral cells. A more likely explanation of our electrophysiological
482 data is based on cannabinoids that activate CB_1 expressed by other MOB cell types such that
483 the observed excitatory effects of CB_1 agonists on mitral cells are indirect. Changes in mitral
484 cell activity are likely to reflect the direct activation of CB_1 on and inhibition of a subpopulation of
485 GAD65-positive GABAergic interneurons in the MOB to regulate the GABA release and
486 inhibitory input to mitral cells. From our experiments with subglomerular slices we conclude that
487 (a) CB_1-mediated effects are limited to the glomerular layer and, therefore, did not involve
488 granule cells, and (b) eCB-mediated regulation involves apical dendrites of mitral cells.
489 Periglomerular cells are multifunctional neurons involved in neuronal circuit dynamics
490 with several partners. Periglomerular cells form synapses onto mitral/tufted cell dendrites
491 (Pinching and Powell, 1971). On the one hand, they play a role in regulating glomerular and
492 bulbar output by synaptically interacting with mitral and tufted cells, while at the same time they
493 have been shown to presynaptically inhibit olfactory afferent input to the MOB (Shipley and
494 Ennis 1996; Ennis et al. 2007). Based on our previous and current results, we postulate that
495 periglomerular cells are candidates for direct modulation by cannabinoids which in turn regulate
496 synaptic input to mitral cells, i.e., sIPSCs, in the periglomerular or, more broadly, GABAergic cell
497 to mitral cell signaling pathway.
498 Periglomerular cells presynaptically inhibit olfactory receptor neuron terminals in the
499 glomerular layer of the MOB (Keller et al. 1998; Hsia et al. 1999; Wachowiak and Cohen 1999;
500 Aroniadou-Anderjaska et al. 2000; Berkowicz and Trombley 2000; Ennis et al. 2001; Palouzier-
501 Paulignan et al. 2002; Murphy et al. 2005). At the same time, olfactory receptor neurons make

direct synaptic contact with mitral and tufted cells (Pinching and Powell 1971). Sensory transmission from olfactory nerve terminals to principal neurons of the MOB, mitral and tufted cells, is mediated by glutamate acting at AMPA and NMDA ionotropic glutamate receptors (Bardoni et al. 1996; Ennis et al. 1996, 2001; Aroniadou-Anderjaska et al. 1997; Chen and Shepherd 1997; Keller et al. 1998). Possibly, besides the signaling pathway from periglomerular cells or other GABAergic cells to mitral cells, CB_1 may indirectly regulate glutamate release from olfactory nerve terminals by relieving presynaptic inhibition of glutamate release. CB_1 could regulate mitral cell activity through another signaling pathway, namely from GABAergic glomerular cells to the olfactory nerve terminals to mitral cells. This hypothesis was supported by our observation that the CB_1 antagonist AM251 increased the frequency of sIPSCs in mitral cells. In this view, eCB release in the glomerular layer inhibits GABAergic cells to reduce GABA release, relieves presynaptic inhibition of olfactory nerve afferents and, subsequently, results in mitral cell excitation. The modulatory effect of CB_1 agonist and antagonist on synaptic transmission to mitral cells supports the hypothesis that cannabinoid effects in mitral cells result from direct CB_1 effects on GABAergic cell processes.

In summary, we have identified components of a cannabinoid signaling system in the MOB and identified a likely interneuron-based circuit that negatively regulates the activity of the main output neurons – the mitral cells. Activation of CB_1 in this circuit will lift the interneuron-mediated inhibition and may render mitral cells more responsive to odor stimulation and synaptic input.

Acknowledgments: We would like to thank Ben Cornett, Alhasan Elghouche, Yun-Hsuan Chou, and Ya-Wen Yang for excellent technical assistance as well as the Indiana University Light Microscopy Imaging Center.

Grants: We thank NIH-NIDA for providing SR141716. This work was supported by the Whitehall Foundation, Latham Trust Fund, NSF (IOS-1355034), and U.S. PHS grants GM08016 to TH, and EY24625 to AS.

References

Alger BE (2002) Retrograde signaling in the regulation of synaptic transmission: focus on endocannabinoids. Prog Neurobiol 68: 247-286.

Alger BE, Kim J (2011) Supply and demand for endocannabinoids. Trends in Neurosci 34:304-315

Allen Institute for Brain Science (2009) Allen Mouse Brain Atlas [Online]. Seattle, WA, 2009. http://mouse.brain-map.org.

Aroniadou-Anderjaska V, Ennis M, and Shipley MT (1999) Current-source density analysis in the rat olfactory bulb: laminar distribution of kainate/AMPA and NMDA receptor-mediated currents. J Neurophysiol 81: 15-28.

Aroniadou-Anderjaska V, Zhou FM, Priest CA, Ennis M, Shipley MT (2000). Tonic and synaptically evoked presynaptic inhibition of sensory input to the rat olfactory bulb via GABA(B) heteroreceptors. J Neurophysiol 84:1194-1203.

Atwood BK, Mackie K CB2 (2010) a cannabinoid receptor with an identity crisis. Br J Pharmacol 160(3):467-79.

Aungst JL, Heyward PM, Puche AC, Karnup SV, Hayar A, Szabo G, Shipley MT (2003) Centre-surround inhibition among olfactory bulb glomeruli. Nature 426: 623-629.

Bardoni R, Puopolo M, Magherini PC, Belluzzi O (1996) Potassium currents in periglomerular cells of frog olfactory bulb in vitro. Neurosci Lett 210:95-98.

Berkowicz DA, Trombley PQ (2000) Dopaminergic modulation at the olfactory nerve synapse. Brain Res 855: 90-99.

Blankman JL, Simon GM, Cravatt BF (2007) A comprehensive profile of brain enzymes that hydrolyze the endocannabinoid 2-arachidonoylglycerol. Chem Biol 14(12):1347-1356.

Bodor AL, Katona I, Nyiri G, Mackie K, Ledent C, Hajos N, et al. (2005). Endocannabinoid signaling in rat somatosensory cortex: laminar differences and involvement of specific interneuron types. J Neurosci 25(29): 6845-6856.

Bracey MH, Hanson MA, Masuda KR, Stevens RC, Cravatt BF (2002). Structural adaptations in a membrane enzyme that terminates endocannabinoid signaling. Science 298(5599): 1793-1796.

Bradshaw HB, Rimmerman N, Hu SS, Benton VM, Stuart JM, Masuda K, et al. (2009). The endocannabinoid anandamide is a precursor for the signaling lipid N-arachidonoyl glycine by two distinct pathways. BMC Biochem 10: 14.

Chang YC, Gottlieb DI (1988). Characterization of the proteins purified with monoclonal antibodies to glutamic acid decarboxylase. J Neurosci 8(6): 2123-2130.

Cravatt BF, Demarest K, Patricelli MP, Bracey MH, Giang DK, Martin BR, et al. (2001). Supersensitivity to anandamide and enhanced endogenous cannabinoid signaling in mice lacking fatty acid amide hydrolase. Proc Natl Acad Sci U S A 98(16): 9371-9376.

Davis BJ, Macrides F (1983) Tyrosine hydroxylase immunoreactive neurons and fibers in the olfactory system of the hamster. J Comp Neurol 214: 427-440.

Devane WA, Hanus L, Breuer A, Pertwee RG, Stevenson LA, Griffin G, et al. (1992). Isolation and structure of a brain constituent that binds to the cannabinoid receptor. Science 258(5090): 1946-1949.

573 Diana MA, Levenes C, Mackie K, Marty A (2002) Short-term retrograde inhibition of GABAergic
574 synaptic currents in rat Purkinje cells is mediated by endogenous cannabinoids. J
575 Neurosci 22:200-208, 2002.
576 Dong HW, Hayar A, Ennis M (2007) Activation of group I metabotropic glutamate receptors on
577 main olfactory bulb granule cells and periglomerular cells enhances synaptic inhibition of
578 mitral cells. J Neurosci 27:5654-5663.
579 Ennis M, Zhou F-M, Ciombor K, Aroniadou-Anderjaska V, Hayar A, Borrelli E, Zimmer LA,
580 Margolis F. Shipley MT (2001) Dopamine D2 receptor-mediated presynaptic inhibition of
581 olfactory nerve terminals. J Neurophysiol 86:2986-2997
582 Ennis M, Zhu M, Heinbockel T, Hayar A (2006) Olfactory nerve-evoked, metabotropic glutamate
583 receptor-mediated synaptic responses in rat olfactory bulb mitral cells. J Neurophysiol
584 95:2233-2241.
585 Ennis, M, Hamilton, KA, and Hayar A (2007) Neurochemistry of the main olfactory system. In:
586 Handbook of Neurochemistry and Molecular Neurobiology (edited by Lajtha A), Sensory
587 Neurochemistry, edited by Johnson DA. Springer: Heidelberg. 137-204.
588 Freund TF, Katona I, Piomelli D (2003) Role of endogenous cannabinoids in synaptic signaling.
589 Physiol Rev 83:1017-1066.
590 Hajos N, Katona I, Naiem SS, MacKie K, Ledent C, Mody I, et al. (2000). Cannabinoids inhibit
591 hippocampal GABAergic transmission and network oscillations. Eur J Neurosci 12(9):
592 3239-3249.
593 Halasz N, Johansson O, Hoekfelt T, Ljungdahl A, Goldstein M (1981) Immunohistochemical
594 identification of two types of dopamine neuron in the rat olfactory bulb as seen by serial
595 sectioning. J Neurocytol 10: 251-259.
596 Harvey JD, Heinbockel T (2018) Neuromodulation of synaptic transmission in the main olfactory
597 bulb. Int J Environ Res Public Health, *15* (10), 2194; doi.org/10.3390/ijerph15102194
598 Hayar A, Heyward P, Heinbockel T, Shipley MT, Ennis M (2001) Direct excitation of mitral cells
599 via activation of α1-noradrenergic receptors in rat olfactory bulb slices. J Neurophysiol
600 86: 2173-2182.
601 Hayar A, Karnup S, Shipley MT, and Ennis M (2004a) Olfactory bulb glomeruli: external tufted
602 cells intrinsically burst at theta frequency and are entrained by patterned olfactory input.
603 J Neurosci 24: 1190-1199.
604 Hayar A, Karnup S, Ennis M, and Shipley MT (2004b) External tufted cells: a major excitatory
605 element that coordinates glomerular activity. J Neurosci 24: 6676-6685.
606 Hayar A, Shipley, MT, and Ennis, M (2005) Olfactory bulb external tufted cells are synchronized
607 by multiple intraglomerular mechanisms. J Neurosci 25: 8197-8208.
608 Heinbockel T, Heyward P, Conquet F, and Ennis M (2004) Regulation of main olfactory bulb
609 mitral cell excitability by metabotropic glutamate receptor mGluR1. J Neurophysiol 92:
610 3085-3096.
611 Hendrickson A, Troilo D, Djajadi H, Possin D, Springer A (2009). Expression of synaptic and
612 phototransduction markers during photoreceptor development in the marmoset monkey
613 Callithrix jacchus. J Comp Neurol 512(2): 218-231.
614 Herkenham M, Lynn AB, Johnson MR, Melvin LS, de Costa BR, Rice KC (1991)
615 Characterization and localization of cannabinoid receptors in rat brain: a quantitative in
616 vitro autoradiographic study. J Neurosci 11:563-583.

617 Heyward P, Ennis M, Keller A, Shipley MT (2001) Membrane bistability in olfactory bulb mitral
618 cells. J Neurosci 21:5311-5320.
619 Hoffman AF, Lupica CR (2000). Mechanisms of cannabinoid inhibition of GABA(A) synaptic
620 transmission in the hippocampus. J Neurosci 20:2470-2479.
621 Howlett AC, Breivogel CS, Childers SR, Deadwyler SA, Hampson RE, Porrino LJ (2004)
622 Cannabinoid physiology and pharmacology: 30 years of progress. Neuropharmacol
623 47:345-358.
624 Hsia AY, Vincent JD, Lledo PM (1999) Dopamine depresses synaptic inputs into the olfactory
625 bulb. J Neurophysiol 82: 1082-1085.
626 Hu SS, Bradshaw HB, Chen JS, Tan B, Walker JM (2008). Prostaglandin E2 glycerol ester, an
627 endogenous COX-2 metabolite of 2-arachidonoylglycerol, induces hyperalgesia and
628 modulates NFkappaB activity. Br J Pharmacol 153(7): 1538-1549.
629 Iannotti FA, Di Marzo V, Petrosino S (2016) Endocannabinoids and Endocannabinoid-Related
630 Mediators: Targets, Metabolism and Role In Neurological Disorders. Prog Lipid Res, pii:
631 S0163-7827(15)30023-0. doi: 10.1016/j.plipres.2016.02.002.
632 Isaacson JS and Strowbridge BW (1998). Olfactory reciprocal synapses: dendritic signaling in
633 the CNS. Neuron 20:749-761.
634 Jevince AR, Kadison SR, Pittman AJ, Chien CB, Kaprielian Z (2006) Distribution of EphB
635 receptors and ephrin-B1 in the developing vertebrate spinal cord. J Comp Neurol 497(5):
636 734-750.
637 Kano M, Ohno-Shosaku T, Hashimotodani Y, Uchigashima M, Watanabe M (2009)
638 Endocannabinoid-mediated control of synaptic transmission. Physiol Rev 89:309-380.
639 Katona I, Sperlagh B, Sik A, Kafalvi A, Vizi ES, Mackie K, Freund TF (1999). Presynaptically
640 located CB1 cannabinoid receptors regulate GABA release from axon terminals of
641 specific hippocampal interneurons. J Neurosci 19:4544-4558.
642 Keller A, Yagodin S, Aroniadou-Anderjaska A, Zimmer LA, Ennis M, Sheppard NF, Shipley MT
643 (1998) Functional organization of rat olfactory bulb glomeruli revealed by optical
644 imaging. J Neurosci 18:2602-2612.
645 Kiyokage E, Pan YZ, Shao Z, Kobayashi K, Szabo G, Yanagawa Y, Obata K, Okano H, Toida
646 K, Puche AC, Shipley MT (2010) Molecular identity of periglomerular and short axon
647 cells. J Neurosci 30:1185-96.
648 Kreitzer AC, Regehr WG (2001a) Retrograde inhibition of presynaptic calcium influx by
649 endogenous cannabinoids at excitatory synapses onto Purkinje cells. Neuron 29:717-
650 727.
651 Leishman E, Cornett B, Spork K, Straiker A, Mackie K, Bradshaw HB (2016a) Broad impact of
652 deleting endogenous cannabinoid hydrolyzing enzymes and the CB1 cannabinoid
653 receptor on the endogenous cannabinoid-related lipidome in eight regions of the mouse
654 brain. Pharmacol Res 110:159-72.
655 Leishman E, Mackie K, Luquet S, Bradshaw HB (2016b) Lipidomics profile of a NAPE-PLD KO
656 mouse provides evidence of a broader role of this enzyme in lipid metabolism in the
657 brain. Biochim Biophys Acta 1861:491-500.
658 Levenes C, Daniel H, Soubrie P, Crepel F (1998) Cannabinoids decrease excitatory synaptic
659 transmission and impair long-term depression in rat cerebellar Purkinje cells. J Physiol
660 (Lond) 510:867-879.

661 Lozovaya N, Yatsenko N, Beketov A, Tsintsadze T, Burnashev N (2005) Glycine receptors in
662 CNS neurons as a target for nonretrograde action of cannabinoids. J Neurosci 25:7499-
663 7506.
664 Lu HC, Mackie K (2016) An introduction to the endogenous cannabinoid system. Biol
665 Psychiatry, 79(7):516-25. doi: 10.1016/j.biopsych.2015.07.028.
666 Maejima T, Hashimoto K, Yoshida T, Aiba A, Kano M (2001) Presynaptic inhibition caused by
667 retrograde signal from metabotropic glutamate to cannabinoid receptors. Neuron 31:463-
668 475.
669 Martin LJ, Blackstone CD, Huganir RL, and Price DL (1992) Cellular localization of a
670 metabotropic glutamate receptor in rat brain. Neuron 9: 259-270.
671 Masu M, Tanabe Y, Tsuchida K, Shigemoto R, Nakanishi S (1991) Sequence and expression of
672 a metabotropic glutamate receptor. Nature 349: 760-765.
673 McLean JH, Shipley MT (1988) Postmitotic, postmigrational expression of tyrosine hydroxylase
674 in olfactory bulb dopaminergic neurons. J Neurosci 8: 3658-3669.
675 Moldrich G, Wenger T (2000) Localization of the CB1 cannabinoid receptor in the rat brain. An
676 immunohistochemical study. Peptides 21:1735-1742.
677 Murphy GJ, Darcy DP, Isaacson JS (2005) Intraglomerular inhibition: Signaling mechanisms of
678 an olfactory microcircuit. Nat Neurosci 8: 354-364.
679 Nyilas R, Dudok B, Urbán GM, Mackie K, Watanabe M, Cravatt BF, Freund TF, Katona I (2008)
680 Enzymatic machinery for endocannabinoid biosynthesis associated with calcium stores
681 in glutamatergic axon terminals. J Neurosci 28: 1058-63.
682 Ohno-Shosaku T, Maejima T, Kano M (2001) Endogenous cannabinoids mediate retrograde
683 signals from depolarized postsynaptic neurons to presynaptic terminals. Neuron 29:729-
684 738.
685 Ohno-Shosaku T, Shosaku J, Tsubokawa H, Kano M (2002) Cooperative eCB production by
686 neuronal depolarization and group I metabotropic glutamate receptor activation. Eur J
687 Neurosci 15:953-961.
688 Okamoto Y, Wang J, Morishita J, Ueda N (2007) Biosynthetic pathways of the endocannabinoid
689 anandamide. Chem Biodivers 4:1842-57.
690 Oveisi F, Gaetani S, Eng KT, Piomelli D (2004). Oleoylethanolamide inhibits food intake in free-
691 feeding rats after oral administration. Pharmacol Res 49(5): 461-466.
692 Palouzier-Paulignan B, Duchamp-Viret P, Hardy AB, Duchamp A. GABA(B) receptor-mediated
693 inhibition of mitral/tufted cell activity in the rat olfactory bulb: A whole-cell patch-clamp
694 study in vitro. Neuroscience 111: 241-250, 2002.
695 Pan B, Wang W, Zhong P, Blankman JL, Cravatt BF, Liu QS (2011). Alterations of
696 endocannabinoid signaling, synaptic plasticity, learning, and memory in
697 monoacylglycerol lipase knock-out mice. J Neurosci 31(38): 13420-13430.
698 Parrish-Aungst S, Shipley MT, Erdelyi F, Szabo G, Puche AC (2007) Quantitative analysis of
699 neuronal diversity in the mouse olfactory bulb. J Comp Neurol 501: 825-836.
700 Pettit DA, Harrison MP, Olson JM, Spencer RF, Cabral GA (1998). Immunohistochemical
701 localization of the neural cannabinoid receptor in rat brain. J Neurosci Res 51:391-402.
702 Pinching AJ, Powell TP (1971) The neuropil of the glomeruli of the olfactory bulb. J Cell Sci 9:
703 347-377.

704 Piomelli D (2003). The molecular logic of endocannabinoid signalling. Nat Rev Neurosci 4(11):
705 873-884.
706 Pouille F, Schoppa NE (2018) Cannabinoid receptors modulate excitation of an olfactory bulb
707 local circuit by cortical feedback. Front Cell Neurosci 12:47. doi:
708 10.3389/fncel.2018.00047. eCollection 2018.
709 Ribak CE, Vaughn JE, Saito K, Barber R, Roberts E (1977) Glutamate decarboxylase
710 localization in neurons of the olfactory bulb. Brain Res 126: 1-18.
711 Ronan PJ, Wongngamnit N, Beresford TP (2016) Molecular Mechanisms of Cannabis Signaling
712 in the Brain. Prog Mol Biol Transl Sci. 137:123-47. doi: 10.1016/bs.pmbts.2015.10.002.
713 Safo PK, Regehr WG (2005) Endocannabinoids control the induction of cerbellar LTD. Neuron
714 48(4):647-659
715 Sahara Y, Kubota T, and Ichikawa M (2001) Cellular localization of metabotropic glutamate
716 receptors mGluR1, 2/3, 5 and 7 in the main and accessory olfactory bulb of the rat.
717 Neurosci. Lett 312: 59-62.
718 Schoppa NE, Kinzie JM, Sahara Y, Segerson TP, and Westbrook GL (1998) Dendrodendritic
719 inhibition in the olfactory bulb is driven by NMDA receptors. J Neurosci 18: 6790-6802.
720 Shao Z, Puche AC, Kiyokage E, Szabo G, Shipley MT (2009) Two GABAergic intraglomerular
721 circuits differentially regulate tonic and phasic presynaptic inhibition of olfactory nerve
722 terminals. J Neurophysiol 101: 1988-2001.
723 Shepherd GW, Chen WR, and Greer CA (2004) Olfactory bulb. In: The Synaptic Organization of
724 the Brain, edited by Shepherd GM. New York: Oxford, 165-216.
725 Shigemoto R., Nakanishi S, and Mizuno N (1992) Distribution of the mRNA for a metabotropic
726 glutamate receptor (mGluR1) in the central nervous system: an in situ hybridization
727 study in adult and developing rat. J Comp. Neurol 322: 121-135.
728 Shipley MT, Ennis M (1996) Functional organization of olfactory system. J Neurobiol 30:123-
729 176.
730 Smart D, Gunthorpe MJ, Jerman JC, Nasir S, Gray J, Muir AI, et al. (2000). The endogenous
731 lipid anandamide is a full agonist at the human vanilloid receptor (hVR1). Br J Pharmacol
732 129(2): 227-230.
733 Soria-Gómez E, Bellocchio L, Reguero L, Lepousez G, Martin C, Bendahmane M, Ruehle S,
734 Remmers F, Desprez T, Matias I, Wiesner T, Cannich A, Nissant A, Wadleigh A, Pape
735 HC, Chiarlone AP, Quarta C, Verrier D, Vincent P, Massa F, Lutz B, Guzmán M, Gurden
736 H, Ferreira G, Lledo PM, Grandes P, Marsicano G (2014) The endocannabinoid system
737 controls food intake via olfactory processes. Nat Neurosci 17(3): 407-15. doi:
738 10.1038/nn.3647.
739 Stella N, Schweitzer P, Piomelli D (1997) A second endogenous cannabinoid that modulates
740 long-term potentiation. Nature 388(6644): 773-778.
741 Straiker A, Mackie K (2009) Cannabinoid signaling in inhibitory autaptic hippocampal neurons.
742 Neuroscience 163(1):190-201.
743 Straiker A, Mackie K (2005) Depolarization-induced suppression of excitation in murine autaptic
744 hippocampal neurones. J Physiol 569(Pt 2): 501-517.
745 Takahashi KA, Linden DJ (2000) Cannabinoid receptor modulation of synapses received by
746 cerebellar Purkinje cells. J Neurophysiol 83:1167-1180.

747 Tamamaki N, Yanagawa Y, Tomioka R, Miyazaki J, Obata K, Kaneko T (2003) Green
748 fluorescent protein expression and colocalization with calretinin, parvalbumin, and
749 somatostatin in the GAD67-GFP knock-in mouse. J Comp Neurol 467(1): 60-79.
750 Tanimura A, Yamazaki M, Hashimotodani Y, Uchigashima M, Kawata S, Abe M, et al. (2010)
751 The endocannabinoid 2-arachidonoylglycerol produced by diacylglycerol lipase alpha
752 mediates retrograde suppression of synaptic transmission. Neuron 65(3): 320-327.
753 Tsou K, Brown S, Sanudo-Pena MC, Mackie K, Walker JM (1998) Immunohistochemical
754 distribution of cannabinoid CB1 receptors in the rat central nervous system.
755 Neuroscience 83:393-411.
756 Valenti M, Vigano D, Casico MG, Rubino T, Steardo L, Parolaro D, et al. (2004) Differential
757 diurnal variations of anandamide and 2-arachidonoyl-glycerol levels in rat brain. Cell Mol
758 Life Sci 61(7-8): 945-950.
759 Van den Pol A. Presynaptic metabotropic glutamate receptors in adult and developing neurons:
760 autoexcitation in the olfactory bulb. J Comp Neurol 359: 253-271, 1995.
761 Varma N, Carlson GC, Ledent C, Alger BE. Metabotropic glutamate receptors drive the eCB
762 system in hippocampus. J Neurosci 21: RC188, 2001.
763 Wachowiak M, Cohen LB (1999) Presynaptic inhibition of primary olfactory afferents mediated
764 by different mechanisms in lobster and turtle. J Neurosci 19: 8808-8817.
765 Wang Z-J, Sun L, Heinbockel T (2012) Cannabinoid receptor-mediated regulation of neuronal
766 activity and signaling in glomeruli of the main olfactory bulb. J Neurosci 32: 8475-8479.
767 Wilson RI, Nicoll RA (2001) Endogenous cannabinoids mediate retrograde signalling at
768 hippocampal synapses. Nature 410:588-592.
769

770 **FIGURE LEGENDS**

771 **Figure 1. CB_1 receptors are present in a sub-population of GAD65-positive periglomerular**
772 **neurons of murine main olfactory bulb. A.** Micrograph shows GAD67-GFP (green) and CB_1
773 staining (red, arrows) in the glomerular layer of the main olfactory bulb. CB_1 and GAD67-GFP
774 staining does not overlap. **A'.** CB_1 staining from A shows that the staining for CB_1 is restricted
775 to a few neuronal processes. EPL – external plexiform layer, glom – glomerulus. **B.** CB_1
776 staining in sample WT and $CB_1^{-/-}$ tissue taken at same setting. **C.** Micrograph shows rare
777 process extending to the external plexiform layer. **D.** Costaining of CB_1 (red, arrows) and
778 recoverin (green) shows that the CB_1 staining is concentrated in periglomerular zone. **E.**
779 GAD67-GFP and CB_1 staining in mitral layer (m - mitral cell) shows an absence of prominent
780 staining in and around these neurons. **F.** Projection of a Z series of GAD65 (green) and CB_1
781 (red) staining shows a long overlapping process (overlap in yellow, arrows). **G.** Higher
782 magnification from F (3 x 230nm sections flattened, rotated 90 degrees clockwise) shows region
783 of clear overlap for GAD65 (green) and CB_1 (red). **G'**, **G''.** CB_1 and GAD65 staining from G.
784 Scale bars: A: 30 μm; B: 20 μm; C: 35 μm; D: 20 μm; E: 10 μm; F: 10 μm; G: 5 μm.
785
786 **Figure 2. Endocannabinoid levels in murine main olfactory bulb. A.** Bar graph shows 2-
787 arachidonoyl glycerol (2-AG) level measured in murine main olfactory bulb. **B.** Anandamide
788 (AEA) level, Oleoyl ethanolamide (OEA) level, Palmitoyl ethanolamide (PEA) level, Stearoyl
789 ethanolamide (SEA) level, Docosahexaenoyl ethanolamide (DHEA) level.
790
791 **Figure 3. RT-PCR measurement of the expression of 12 cannabinoid-related genes in**
792 **murine main olfactory bulb.** GAPDH is a housekeeping gene as an internal control. The
793 PCR products were examined on 1% agarose gel with EtBr. CB_1 & CB_2: cannabinoid receptor 1
794 & 2; NAPE-PLD: *N*-acyl-phosphatidylethanolamine-hydrolyzing phospholipase D; GDE1:
795 glycerophosphodiesterase 1; FAAH: fatty acid amide hydrolase, NAAA: *N*-acylethanolamine-

hydrolyzing acid amidase; DGLα/β: diacylglycerol lipase α/β; MGL: monoacylglycerol lipase; ABHD4/6/12: α/β-hydrolase domain 4/6/12.

Figure 4. The activity of mitral cells was regulated by cannabinoids. A. Original recording illustrates the increased firing rate of a mitral cell in response to bath application of CB_1 agonist AEA (10 μM). Time points 1 and 2 in the upper trace are shown at higher time resolution in the second and third trace, resp. **B.** Representative mitral cell depolarized by AEA (10 μM) . **C.** Original recording from a mitral cell displayed the reduction in firing rate and hyperpolarization following application of CB_1 antagonist AM251. **D.** Representative mitral cell with hyperpolarized membrane potential in response to AM251 . **E.** Group data of the effect of CB_1 agonists and antagonist AM251 on spike rate. Asterisks indicate significance level (* - $p < 0.05$, ** - $p < 0.01$, *** - $p < 0.001$).

Figure 5. Effects of cannabinoids on sIPSCs in mitral cells. A. Original recording from a representative mitral cell shows an increase of sIPSCs in response to AM251 and the development of an outward current. Currents were recorded using a low-Cl^- pipette solution mode. Holding potential was 0 mV. sIPSCs were upward. **B, C.** Original recording shows that AM251 increased and WIN decreased the frequency of sIPSCs in a representative mitral cell in the presence of CNQX plus AP5. Currents were recorded at a holding potential of -60 mV using high-Cl^--based (CsCl) pipette solution. sIPSCs were inward (downward) in this recording condition. The trace in **C** is shown at an extended time scale in the lower traces **(a)** and **(b)**. The arrows in the upper trace indicate the starting point of traces **(a)** and **(b)**. **D.** The cumulative data of the effect of AM251 and WIN on sIPSCs recorded from mitral cells. Asterisks indicate significance level (* - $p < 0.05$, ** - $p < 0.01$).

Figure 6. CB_1 failed to modulate mitral cell activity in subglomerular slices. A. Mitral cell apical dendrite from regular slice stained with Lucifer Yellow. **B.** Mitral cell from a subglomerular slice in which the apical tuft of the mitral cell is not present. Bar = 200 um. **C, D.** Original recordings show lack of CB_1 effect on mitral cell activity in subglomerular slices. Neither CB_1 antagonist AM251 (**C**) nor agonist WIN (**D**) modulated mitral cell spiking rate.

Figure 7. The effect of a CB_1 agonist and an antagonist on mitral cells in the presence of fast synaptic blockers. A. Original recording shows no effect of CB_1 agonist WIN on firing rate and membrane potential in the presence of blockers of fast synaptic transmission [synaptic blockers: CNQX (10 μM), APV (50 μM), and gabazine (5 μM)]. **B.** Original recording showed that AM251 failed to reduce the mitral cell spike rate in fast synaptic blockers.

Figure 8. Diagram of the glomerular network. A. Olfactory nerve (ON) afferents enter the main olfactory bulb through the olfactory nerve laver to synapse with periglomerular cells (PG), mitral cells (MC) and tufted cells (of which only external ones, eTCs are shown) within the glomerular layer. Periglomerular cells inhibit olfactory nerve terminals, external tufted cells and mitral cells. The processes of Short Axon (SA) cells, which are GABAergic and dopaminergic, receive excitatory synaptic input and form extensive interconnections between glomeruli. Mitral cell apical dendrites convey sensory information to deeper layers of the main olfactory bulb. Mitral cells and tufted cells form dendrodenritic synapses with glomerular neuronal processes. B. Dendrodendritic interactions of mitral cells and periglomerular cells. Cannabinoids are released non-synaptically by mitral and potentially other cells act on cannabinoid receptors in periglomerular cells to modulate their synaptic release of GABA. Only the apical dendrite of the mitral cell is shown. GABAR – GABA

845 receptors, GluR – ionotropic and metabotropic glutamate receptors. Panel A is modified
846 from Harvey and Heinbockel (2018) with permission of the publisher MDPI.

Table 1: Primers designed for assorted mouse cannabinoid-related genes

Gene	NCBI Reference	Primer Name	Sequence (5'-3')	Position	Size (bp)
CB_1	NM_007726.3	CB_1-Forward	CTGATCCTGGTGGTGTTGATCATCTG	1631-1993	363
		CB_1-Reverse	CGTGTCTGTGGACACAGACATGGT		
CB_2	BC024052.1	CB_2-Forward	CCTGGGATAGCTCGGATGCG	821-1167	347
		CB_2-Reverse	GTGGTTTTCACATCAGCCTCTGTTTC		
NAPE-PLD	NM_178728.5	NAPE-PLD-Forward	GGGTTTCGACTTCTCGCCGAGGG	133-528	396
		NAPE-PLD-Reverse	CCAGCCTCTCTCACTCCAGCGT		
ABHD4	NM_134076.2	ABHD4-Forward	CCGGCAGGGCTTGTTTACTA	47-391	345
		ABHD4-Reverse	GAGCTTCGCCCAAAACCAAG		
GDE1	NM_019580.4	GDE1-Forward	GGATTTTGTCTCCCCGGACT	922-1262	341
		GDE1-Reverse	AAGTGTGGAGCCTTCCTTGG		
FAAH	NM_010173.4	FAAH-Forward	TAGCCTGGCATTGTGCATGA	1109-1446	338
		FAAH-Reverse	AGCAGGGATCCACAAAGTCG		
NAAA	NM_025972.4	NAAA-Forward	TGGCGCAGGTCATTGGCGAC	255-498	244
		NAAA-Reverse	TCCAGGTTCCGGCCGTGGTAA		
DGLα	NM_198114.2	DGLα-Forward	GACGAGGGCCACCTGTTTTA	2552-2851	300
		DGLα-Reverse	CTCGGCGAATTCTAGCACCT		
DGLβ	NM_144915.3	DGLβ-Forward	TGTTGGTACGGACTGTTCGG	1780-2114	335
		DGLβ-Reverse	ACGTCAGGCATGTGGTCAAT		
MGL	NM_001166251.1	MGL-Forward	TTTCCTTCCCTAAGCGGTCG	102-437	336
		MGL-Reverse	CCACAGCCTCGAGTATCAGC		
ABHD6	NM_025341.3	ABHD6-Forward	AAGTTCGCTACGCACACCAT	242-574	333
		ABHD6-Reverse	AAGCGGCATATACTCCAGCC		
ABHD12	NM_024465.3	ABHD12-Forward	TGTCTGGTGGAAGAATGCCC	622-956	335
		ABHD12-Reverse	GCCGTACCAGATTTGTTGCC		
GAPDH	AK147969.1	GAPDH-Forward	GGGAAGCTCACTGGCATGGC	736-1039	304
		GAPDH-Reverse	GGTCCACCACCCTGTTGCT		

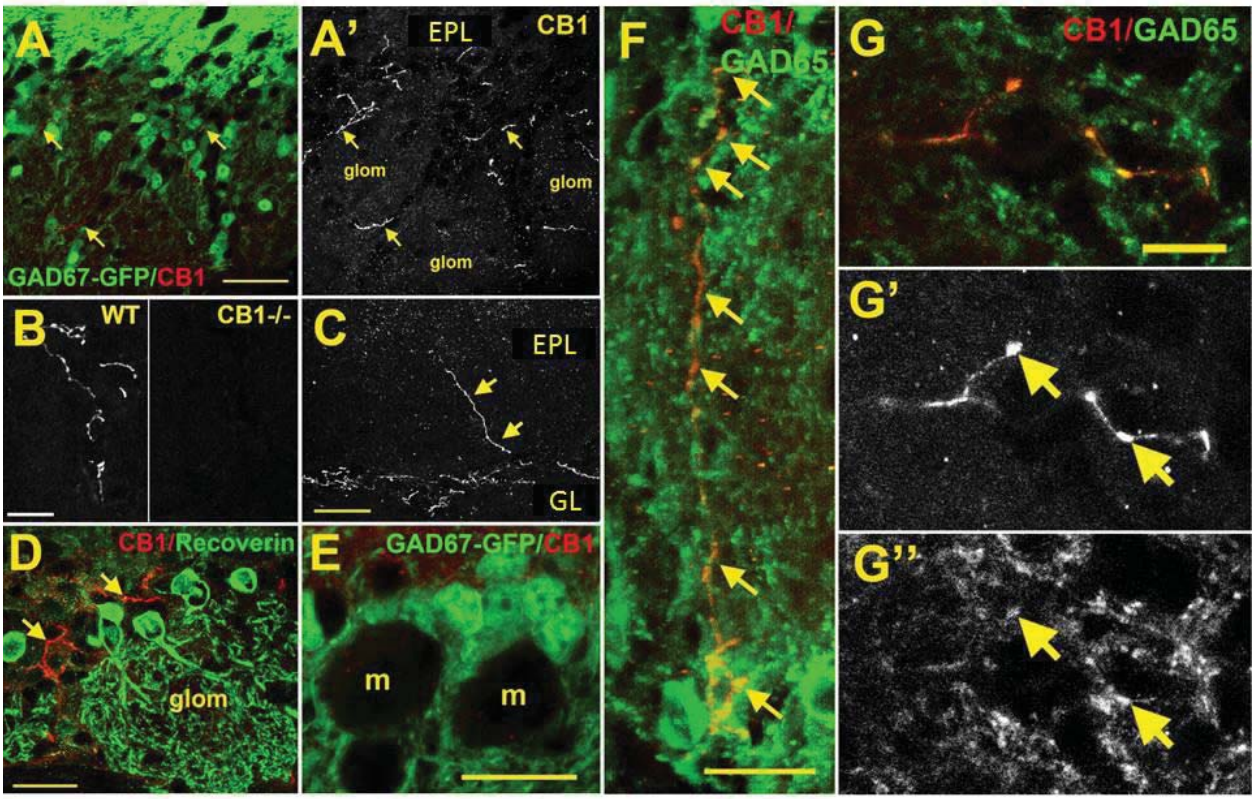

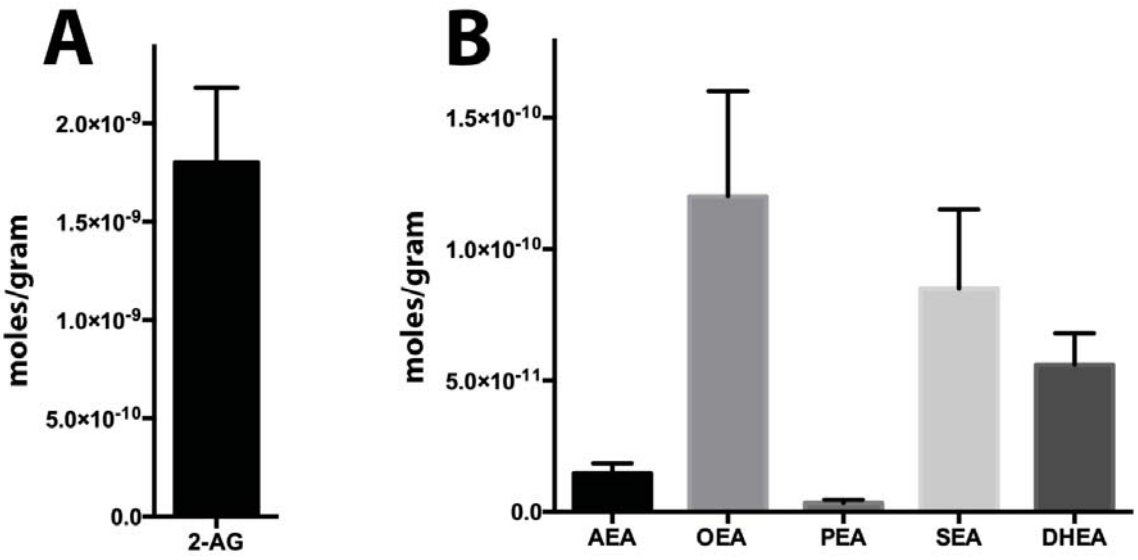

Figure 3

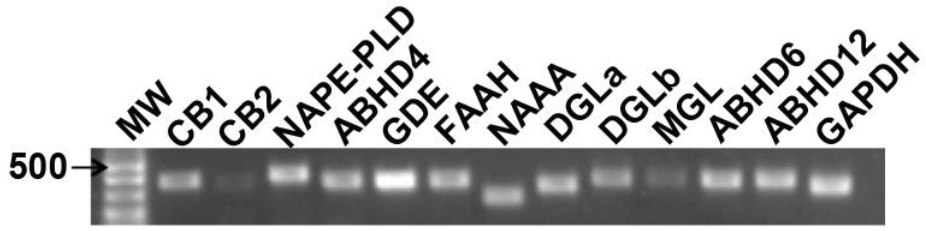

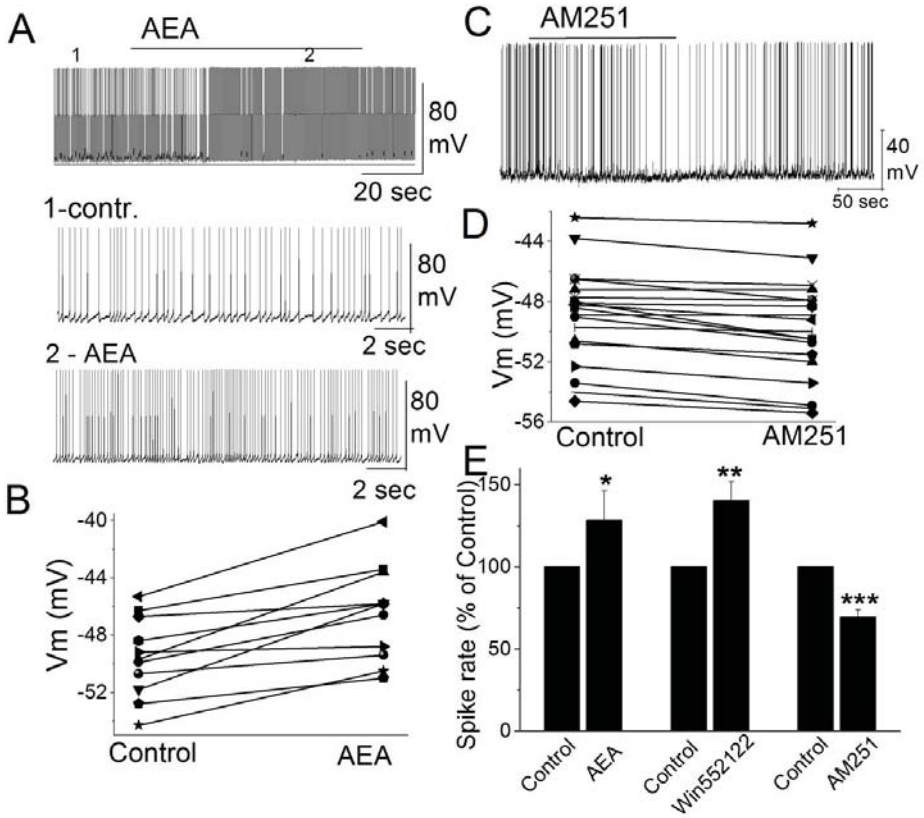

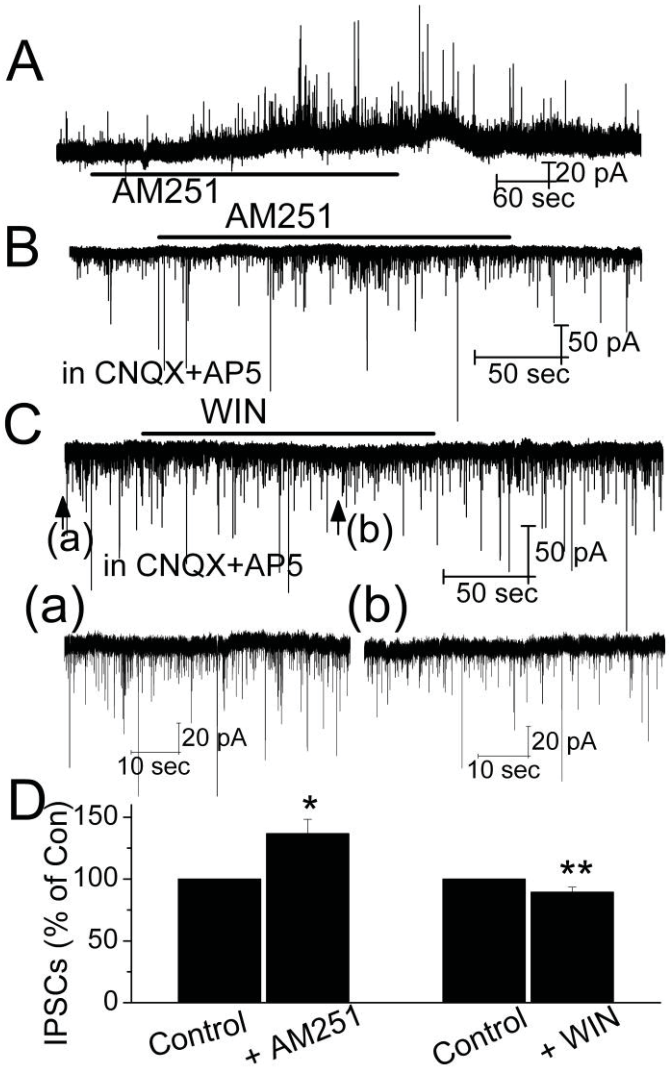

Figure 6